Original Article

JCBFM

Journal of Cerebral Blood Flow & Metabolism
2017, Vol. 37(3) 877–889

DOI: 10.1177/0271678X16646788
journals.sagepub.com/home/jcbfm
SAGE

Depiction of microglial activation in aging and dementia: Positron emission tomography with [^{11}C]DPA713 versus [^{11}C](*R*)PK11195

Masamichi Yokokura[1], Tatsuhiro Terada[2], Tomoyasu Bunai[2], Kyoko Nakaizumi[1], Kiyokazu Takebayashi[1], Yasuhide Iwata[1], Etsuji Yoshikawa[3], Masami Futatsubashi[3], Katsuaki Suzuki[1], Norio Mori[1] and Yasuomi Ouchi[2]

Abstract

The presence of activated microglia in the brains of healthy elderly people is a matter of debate. We aimed to clarify the degree of microglial activation in aging and dementia as revealed by different tracers by comparing the binding potential (BP_{ND}) in various brain regions using a first-generation translocator protein (TSPO) tracer [^{11}C](*R*)PK11195 and a second-generation tracer [^{11}C]DPA713. The BP_{ND} levels, estimated using simplified reference tissue models, were compared among healthy young and elderly individuals and patients with Alzheimer's disease (AD) and were correlated with clinical scores. An analysis of variance showed category-dependent elevation in levels of [^{11}C]DPA713 BP_{ND} in all brain regions and showed a significant increase in the AD group, whereas no significant changes among groups were found when [^{11}C](*R*)PK11195 BP_{ND} was used. Cognito-mnemonic scores were significantly correlated with [^{11}C]DPA713 BP_{ND} levels in many brain regions, whereas [^{11}C](*R*)PK11195 BP_{ND} failed to correlate with the scores. As mentioned elsewhere, the present results confirmed that the second-generation TSPO tracer [^{11}C]DPA713 has a greater sensitivity to TSPO in both aging and neuronal degeneration than [^{11}C](*R*)PK11195. Positron emission tomography with [^{11}C]DPA713 is suitable for the delineation of in vivo microglial activation occurring globally over the cerebral cortex irrespective of aging and degeneration.

Keywords

Aging, brain imaging, dementia, microglia, positron emission tomography

Received 25 August 2015; Revised 21 March 2016; Accepted 30 March 2016

Introduction

Microglial activation accompanies any damage of the brain milieu caused by not only neuronal injuries but also by normal aging-related changes in the brain tissue.[1,2] Activated microglia play a major role in the neuroinflammatory response in the brain and represent an important marker of neuroinflammation.[3] It has also been reported that age-related activation of microglia is linked to an impairment in cognitive function in animals and humans.[2,4,5] A biochemical study showed a significant relationship between cognitive decline and abnormal levels of proinflammatory cytokines, which may underlie the role of activated microglia in the brain and cognitive decline with age.[6]

[1]Department of Psychiatry and Neurology, Hamamatsu University School of Medicine, Hamamatsu, Japan
[2]Department of Biofunctional Imaging, Hamamatsu University School of Medicine, Hamamatsu, Japan
[3]Central Research Laboratory, Hamamatsu Photonics K.K., Hamamatsu, Japan

Corresponding author:
Yasuomi Ouchi, Department of Biofunctional Imaging, Medical Photonics Research Center, Hamamatsu University School of Medicine, 1-20-1 Handayama, Higashi-ku, Hamamatsu 431-3192, Japan.
Email: ouchi@hama-med.ac.jp

Because microglial activation develops over the course of the aging process, microglial activation concomitant with neuronal death is expected in the brains of patients with Alzheimer's disease (AD).[7] It has also been reported that immunological markers, major histocompatibility complex II (MHC II) and CD11b are related to microglial activation during normal aging.[8] The CD45 protein was found to be a marker of activated microglia involved in neurodegenerative diseases, including AD.[9] Aside from neurodegeneration, a recent neuroinflammation study on developmental disorders such as autism also suggested an increase in microglial activation in vivo.[10] Therefore, a clear delineation of activated microglia in normal aging and in brain disorders is important for not only pathophysiology but also for pharmacological intervention studies.

The 18-kDa translocator protein (TSPO), formerly known as the peripheral benzodiazepine receptor or PBR, is a protein located on the outer mitochondrial membrane that is expressed in glial cells.[1,3] A postmortem study revealed that TSPO was highly expressed in CD68-labeled activated microglia in various neurological diseases.[11] In an in vivo research setting, positron emission tomography (PET) could specifically delineate the TSPO density in activated microglia.[11] A first-generation TSPO tracer, [^{11}C](*R*)PK11195, has been extensively used with PET to evaluate microglial activation in vivo in a variety of diseases.[10–13] Previous in vivo [^{11}C](*R*)PK11195 PET studies demonstrated an increased TSPO density accompanying normal aging of the brain.[14] The microglial activation measured by this first-generation TSPO tracer, [^{11}C](*R*)PK11195, reportedly paralleled cognitive deterioration.[12,15] However, [^{11}C](*R*)PK11195 was reported to suffer from high nonspecific binding and a low signal-to-noise ratio. Because of the inability to detect subtle changes of [^{11}C](*R*)PK11195 uptake during the aging process, it might be difficult to evaluate changes in TSPO overexpression under conditions of presymptomatic or early cognitive decline. In addition, some PET studies with [^{11}C](*R*)PK11195 reported a lack of a significant correlation between TSPO overexpression and cognitive severity.[16,17]

In recent years, second-generation TSPO candidate tracers have been developed and tested through preclinical experiments and are now being evaluated in clinical settings. PET studies in AD patients using [^{11}C]DAA1106, [^{11}C]PBR28, [^{11}C]vinpocetine, [^{18}F]FEDDA, and [^{18}F]DPA714 have been reported.[18–22] Although the short half-life of [^{11}C]-labeled tracers limits their applicability in the clinic, [^{11}C]DAA1106 and [^{11}C]PBR28 PET studies showed significantly increased TSPO overexpression in AD patients,[18,19] but a significant correlation between TSPO overexpression and cognitive severity was found only in the [^{11}C]PBR28 PET study.[19] However, these results did not take into account multiple statistical comparisons. There is a need to investigate regional changes in TSPO overexpression with a robust significance level, which will require PET studies on multiple regions of the brain to assess activated microglia development as measured by TSPO overexpression in terms of β-amyloid generation in the AD brain. An animal study showed that [^{11}C]DPA713 had a higher signal-to-noise ratio than [^{11}C](*R*)PK11195.[23] A preliminary study in humans also showed higher trends for specific uptake of [^{11}C]DPA713 compared with [^{11}C](*R*)PK11195.[24] In addition, [^{11}C]DPA713 had a similar or relatively higher order of binding capacity relative to [^{11}C]DAA1106 and [^{11}C]PBR28.[24] Taking genotypic differences in TSPO tracers into account, the use of [^{11}C]DPA713 also has merit among Asians, who manifest almost uniform genotyping for the second-generation TSPO tracers (http://hapmap.ncbi.nlm.nih.gov/cgi-perl/snp_details_phase3?name=rs6971&source=hapmap28_B36&tmpl=snp_details_phase3).[25] To examine the applicability of [^{11}C]DPA713 in revealing microglial activation as measured by TSPO density in terms of cognitive relevance in normal aging and degeneration, we estimated the binding potential (BP_{ND}) of [^{11}C]DPA713 in young and elderly subjects and AD patients and compared the difference of the BP_{ND} among the three groups with the BP_{ND} of [^{11}C](*R*)PK11195. We also examined molecular–clinical relationships based on [^{11}C]DPA713 binding and the clinical parameters in these three groups.

Materials and methods

Participants

Thirteen healthy young subjects (mean age ± SD, 21.5 ± 1.8 years), 12 healthy elderly subjects (71.6 ± 2.6 years, mean Mini-Mental State Examination (MMSE) score ± SD, 28.3 ± 1.0), and 7 patients with AD (69.3 ± 7.4 years, MMSE 19.4 ± 2.7) participated in the [^{11}C]DPA713 PET study (Table 1). In a different group, 13 healthy young subjects (mean age 21.4 ± 2.0 years), 10 healthy elderly subjects (72.2 ± 8.1 years, MMSE 29.5 ± 0.9), and 10 patients with AD (70.8 ± 6.7 years, MMSE 22.1 ± 3.3) participated in the [^{11}C](*R*)PK11195 PET study (Table 1). All participants were Japanese. We used a t-test to compare ages and MMSE scores among all participants in each group. There was no significant difference in the age of the elderly subjects and AD patients in either group. MMSE scores of AD patients were significantly lower than those of elderly subjects in both the [^{11}C]DPA713 and [^{11}C](*R*)PK11195 PET groups, but no significant difference was found between the two AD groups. The diagnosis of AD was based on the criteria of the National Institute of Neurological and

Table 1. Participants.

[^{11}C]DPA713 group									[^{11}C](*R*)PK11195 group							
	Young group (n = 13)		Elderly group (n = 12)			AD group (n = 7)			Young group (n = 13)		Elderly group (n = 10)			AD group (n = 10)		
	Age	Sex	Age	Sex	MMSE	Age	Sex	MMSE	Age	Sex	Age	Sex	MMSE	Age	Sex	MMSE
	21	M	73	M	30	76	F	21	21	M	59	F	30	76	M	24
	20	M	67	F	29	66	F	20	21	M	60	F	30	70	F	18
	21	M	71	F	28	71	F	17	22	M	84	M	29	62	F	23
	23	M	66	M	27	61	F	14	22	M	70	F	30	81	M	25
	20	M	72	M	28	80	F	21	22	M	74	F	30	57	M	25
	22	M	71	F	30	58	M	22	21	M	69	F	30	74	F	22
	21	M	72	F	27	73	F	21	22	M	85	F	27	69	F	23
	21	M	74	M	29				22	M	76	M	30	69	F	20
	22	M	72	F	28				21	M	73	M	29	75	M	15
	20	M	74	F	29				19	M	72	M	30	75	M	26
	20	M	72	F	28				19	M						
	21	M	75	M	27				19	M						
	27	M							27	M						
Mean	21.5[a]		71.6		28.3[b]	69.3		19.4	21.4[c]		72.2		29.5[d]	70.8		22.1
sd	1.9		2.7		1.1	8.0		2.9	2.1		8.6		1.0	7.1		3.5

[a]$p < 0.05$, vs. elderly and AD groups in the [^{11}C]DPA713 group. [b]$p < 0.05$, vs. AD group in the [^{11}C]DPA713 group. [c]$p < 0.05$, vs. elderly and AD groups in the [^{11}C](*R*)PK11195 group. [d]$p < 0.05$, vs. AD group in the [^{11}C](*R*)PK11195 group.

Communicative Disorders and Stroke-Alzheimer's Disease and Related Disorders Association (NINCDS/ADRDA)[26] and the Diagnostic and Statistical Manual of Mental Disorders-IV (DSM-IV). Prior to their selection, each AD patient underwent a diagnostic 1.5 T or 3 T magnetic resonance imaging (MRI), [^{18}F]FDG and [^{11}C]PIB PET. The results of the diagnostic MRI and PET supported the clinical diagnosis in each case. The exclusion criteria were as follows: (a) the presence of significant white matter microvascular changes on the MRI over and above a few scattered lacunes typical of normal aging, (b) smoking or drinking a significant amount of alcohol regularly, (c) taking nootropic drugs regularly, (d) having untreated hypertension or diabetes, and (e) having a history of neurological and psychiatric disorders other than AD. The neuropsychological assessment for all AD patients was based on the MMSE. The above exclusion criteria except (e) were also applied when selecting healthy young and elderly subjects. Healthy subjects had no neurological or psychiatric disorders. This study was approved by the Ethics Committee of the Hamamatsu Medical Center by abiding by the Ethical Guidelines for Clinical Research (Public Notice of the Japanese Ministry of Health, Labour and Welfare No. 415 of 2008). We obtained written informed consent from all participants. The subjects were informed both verbally and in writing about the objectives, procedures and eventual risks of the experimental procedure.

MRI scanning

MRI was performed to determine the areas of the regions of concern for setting regions of interest (ROIs) using the 1.5 T MRI machine (Signa HDxt, GE, USA) with the following acquisition parameters: three-dimensional mode sampling, TR/TE (25/Minimum), 30° flip angle, 1.5 mm slice thickness with no gap, and 256 × 128 matrices. The MRI parameters and a mobile PET gantry allowed us to reconstruct the PET images parallel to the intercommissural (ACPC) line without reslicing; using this approach, we were able to allocate ROIs on the target regions of the original PET images.[27]

PET data acquisition

Participants underwent [^{11}C]DPA713 or [^{11}C](*R*)PK11195 PET measurements after MRI scanning. We used a high-resolution brain PET scanner (SHR12000, Hamamatsu Photonics K.K., Hamamatsu, Japan), which was capable of yielding 47 tomographic images.[28] A 10-min transmission scan for attenuation correction using a ^{68}Ge/^{68}Ga source was conducted with the subject's head fixed by a radiosurgery-purpose thermoplastic

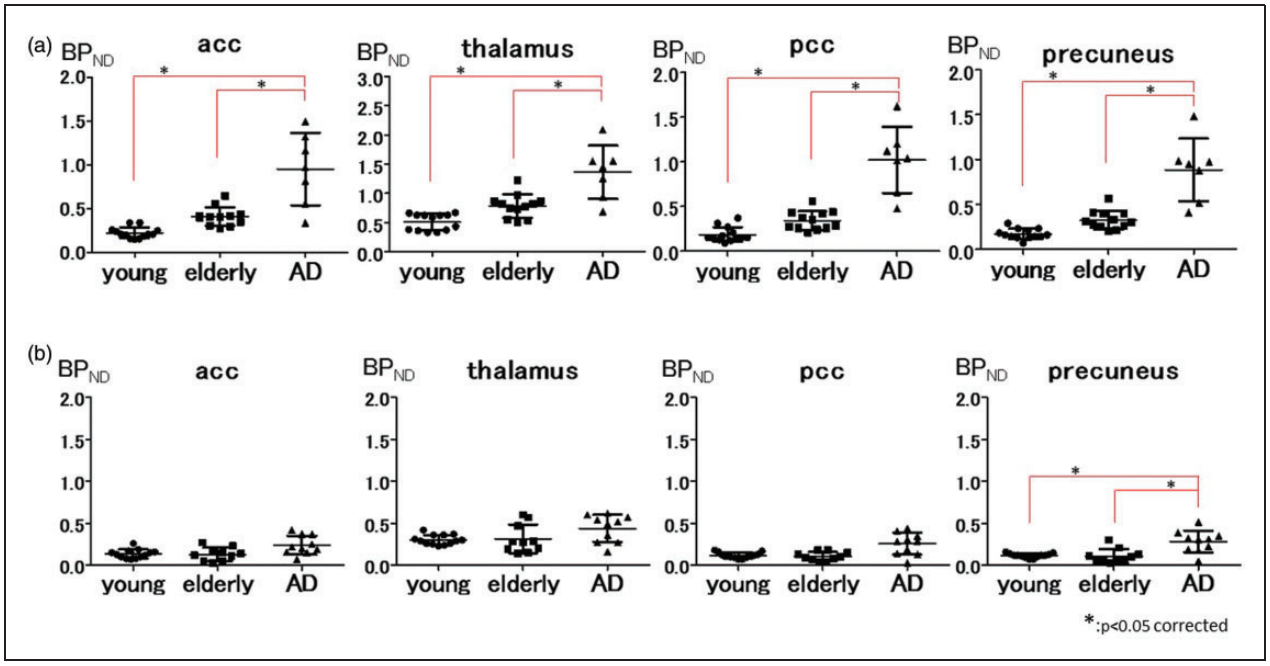

Figure 1. Representative regional BP_{ND} values in the healthy young, healthy elderly, and AD groups using the input curve from young subjects. In the AD group, BP_{ND} values are significantly higher in extensive brain regions than in the young and elderly groups in the [^{11}C]DPA713 study (a), whereas BP_{ND} values of [^{11}C](*R*)PK11195 are significantly higher in the precuneus (b). The asterisk (*) indicates $p < 0.05$, corrected for multiple comparisons.
acc: anterior cingulate cortex; pcc: posterior cingulate cortex.

facemask under resting conditions. After backprojection and filtering (Hanning filter, cut-off frequency 0.2 cycles per pixel), the image resolution was $2.9 \times 2.9 \times 3.4$ mm^3 FWHM. The voxel of each reconstructed image measured $1.3 \times 1.3 \times 3.4$ mm^3. After an intravenous injection of [^{11}C]DPA713 (mean dose 286 ± 50 MBq) or [^{11}C](*R*)PK11195 (mean dose 312 ± 64 MBq), dynamic PET scans with 32 frames (time frames: 4×30, 20×60, and 8×300 s) were performed for 62 min.

Image data processing

The binding potential (BP_{ND}) of [^{11}C]DPA713 and [^{11}C](*R*)PK11195 was estimated based on a simplified reference tissue model (SRTM)[29] in which we used a normalized mean time activity curve based on young subjects as a reference tissue curve. This procedure has been described elsewhere.[13] Briefly, a normalized input curve was created by averaging the ROIs placed over the bilateral frontal cortex, temporal cortex, parietal cortex, occipital cortex, thalamus, basal ganglia, and cerebellar hemisphere in the young subjects. The normalized mean tissue activity curve was then used as the reference input function because a desirable reference region free from specific binding is not present in patients with neurodegenerative disorders. The normalized input curve derived from the young subjects was used as the time–activity curve for the reference region of the young subjects, elderly subjects, and AD patients. To create a validation for the present method using the input curve from young subjects, we also analyzed data two ways using an input curve from elderly subjects and a clustered input curve extracted from gray matter without specific binding.[30] As shown in Figure 1, supplementary figures 1, 3, and 5, we showed here that using the young group as reference input provided comparable results to clustered analysis for [^{11}C]DPA713. However, the clustered analysis seemed to be more sensitive for [^{11}C](*R*)PK11195, as illustrated by the number of ROIs in which a significant difference between elderly subjects and AD patients could be detected (Figure 1, supplementary figure 2, 4 and 6). All BP_{ND} parametric PET images were generated using PMOD 3.2 software (PMOD Technologies Ltd., Switzerland).

Image data analysis and statistics

ROI analysis

ROIs were manually drawn bilaterally over the cerebellum hemisphere, hippocampus, parahippocampal cortex (phc), amygdala, anterior cingulate cortex (acc), caudate nucleus, putamen, thalamus, posterior cingulate cortex (pcc), precuneus, superior frontal cortex (sfc) (Brodmann area or BA 9), middle frontal cortex (mfc)

Table 2. Regional BP_{ND} values for [^{11}C]DPA713 and [^{11}C](*R*)PK11195.

Region	[^{11}C]DPA713 BP						[^{11}C](*R*)PK11195 BP					
	Young group		Elderly group		AD group		Young group		Elderly group		AD group	
	Mean	sd	Mean	sd	Mean	sd	Mean	sd	Mean	sd	Mean	sd
Cerebellum	0.22	0.08	0.38	0.15	0.87[a]	0.31	0.16	0.05	0.13	0.10	0.23	0.14
Hippocampus	0.21	0.09	0.37	0.09	1.01[a]	0.39	0.15	0.05	0.18	0.17	0.21	0.11
Phc	0.16	0.08	0.30	0.09	0.89[a]	0.40	0.11	0.05	0.12	0.12	0.26	0.10
Amygdala	0.28	0.12	0.47	0.14	1.18[a]	0.59	0.17	0.09	0.19	0.15	0.33	0.19
Acc	0.23	0.06	0.41	0.10	0.95[a]	0.38	0.12	0.05	0.13	0.08	0.24	0.11
Caudate	0.11	0.06	0.20	0.05	0.65[a]	0.24	0.08	0.03	0.10	0.14	0.15	0.11
Putamen	0.20	0.07	0.40	0.13	0.85[a]	0.32	0.15	0.05	0.18	0.11	0.27	0.10
Thalamus	0.51	0.14	0.79	0.19	1.36[a]	0.42	0.30	0.06	0.32	0.16	0.44	0.15
Pcc	0.19	0.08	0.34	0.10	1.02[a]	0.34	0.11	0.03	0.11	0.05	0.26	0.13
Precuneus	0.17	0.06	0.33	0.10	0.88[a]	0.32	0.12	0.03	0.11	0.08	0.28[b]	0.12
Sfc	0.12	0.06	0.26	0.08	0.87[a]	0.33	0.09	0.04	0.08	0.09	0.21	0.12
Mfc	0.17	0.07	0.29	0.06	0.93[a]	0.39	0.12	0.04	0.11	0.08	0.23	0.10
Lat temporal ctx	0.07	0.03	0.25	0.08	0.85[a]	0.28	0.14	0.06	0.14	0.15	0.27	0.15
Occipital ctx	0.12	0.06	0.27	0.10	0.87[a]	0.34	0.15	0.07	0.14	0.08	0.27	0.14
Lat parietal ctx	0.13	0.05	0.25	0.09	1.01[a]	0.63	0.11	0.04	0.13	0.11	0.26	0.14

[a]$p < 0.05$ corrected, vs. both young and elderly groups in the [^{11}C]DPA713 group. [b]$p < 0.05$ corrected, vs. both young and elderly groups in the [^{11}C](*R*)PK11195 group.

(BA9), lateral temporal cortex, occipital cortex, and lateral parietal cortex on the ACPC-aligned MR images of each subject. The delineated ROIs were placed on the same area on both the MR and the corresponding PET images. Both reconstructed PET and MR images were obtained parallel to the intercommissural line.[13] These ROIs were transferred onto the corresponding quantitative BP_{ND} parametric PET images. We made direct comparisons with BP_{ND} values obtained across multiple ROIs among young subjects, elderly subjects, and AD patients in each PET tracer using one-way ANOVA. To compare the degree of binding capacity of [^{11}C]DPA713 with that of [^{11}C](*R*)PK11195 in the AD subjects, a BP ratio index was calculated by dividing the BP_{ND} of each brain region in the AD subjects by the mean BP_{ND} of the same brain region in the elderly subjects. Then, we compared the [^{11}C]DPA713 BP_{ND} ratio with the [^{11}C](*R*)PK11195 BP_{ND} ratio. BP_{ND} data from elderly subjects and AD patients were used for comparison between BP_{ND} levels and MMSE scores in each delineated brain region using Pearson's correlation and simple regression analyses with statistical significance set at $p < 0.05$ corrected for multiple comparisons (SPSS version 21; SPSS Japan Inc., Tokyo).

SPM analysis

We examined the whole brain using a voxel-wise analysis in SPM8 (Wellcome Department of Cognitive Neurology, London, UK, http://www.fil.ion.ucl.ac.uk/spm/software/spm8/). All [^{11}C]DPA713 and [^{11}C](*R*)PK11195 BP_{ND} parametric images were first normalized to the Montreal Neurological Institute space and smoothed with an isotropic Gaussian kernel of 8 mm. The between-group comparisons (AD patients vs. elderly subjects and elderly subjects vs. young subjects) for each parameter were performed using t statistics on a voxel-by-voxel basis with a statistical threshold set at $p < 0.001$, where age served as the confounding covariate in the comparison between AD and healthy elderly subjects. When evaluating the age-related difference in TSPO density, age did not serve as a confounding covariate in the comparison between elderly and young subjects.

Results

Group comparison

All our results except for Table 1, supplementary figures 1, 2, 3, and 4 were generated using the input curve from young subjects. Table 1 was characteristics of participants. Supplementary figures 1 and 2 were generated using the input curve from elderly subjects. Supplementary figures 3 and 4 were generated by the clustered input curve. Statistical results in ROI-based analyses on BP_{ND} values grouped by young subjects, elderly subjects, and AD patients are shown in Figure 1 and supplementary figures 5 and 6. Regional BP_{ND}

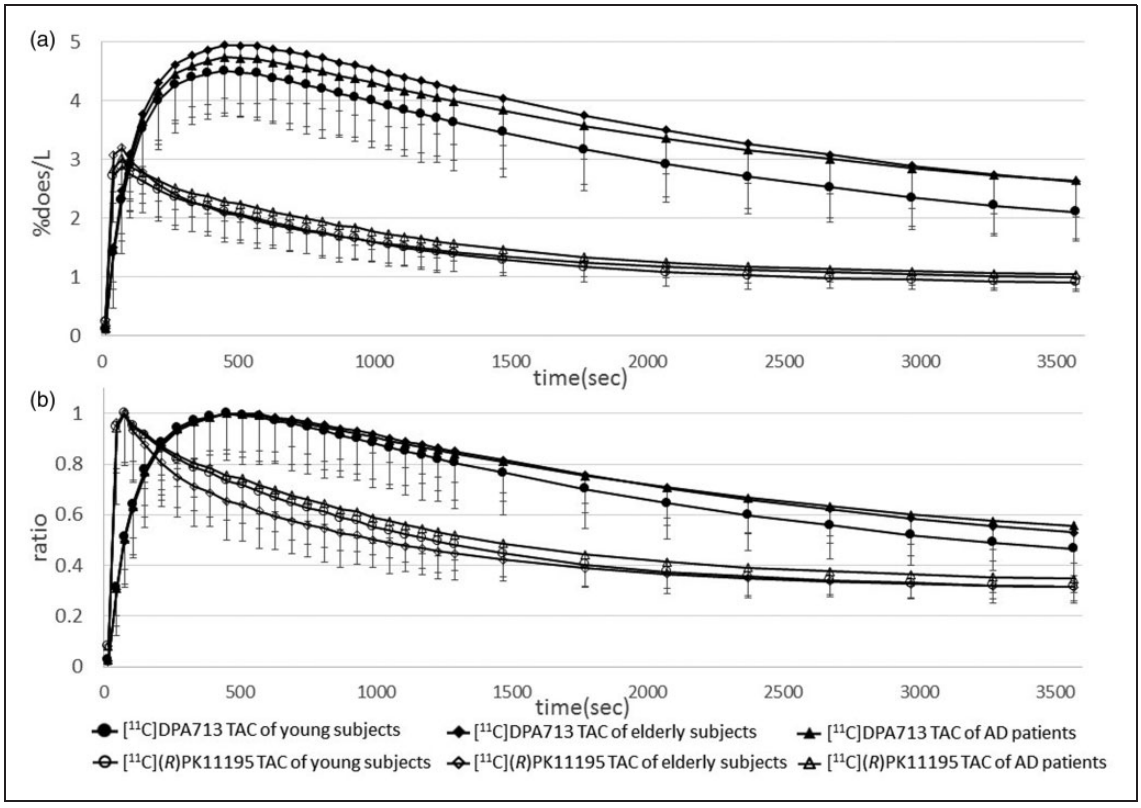

Figure 2. Radiotracer time activity curves (TACs) derived from young subjects of [^{11}C]DPA713 and [^{11}C](*R*)PK11195 in the precuneus. The abscissa indicates the time. The ordinates indicate %dose/L in Figure 2(a) and a unitless ratio in Figure 2(b), where the ratio was calculated by dividing the value of each TAC by the peak value of the same TAC. The ratio of TACs show a clear separation of the [^{11}C]DPA713 TACs among the three groups compared with those of the [^{11}C](*R*)PK11195 TACs during the late retention period.

values for both radioligands are displayed in Table 2. The levels of [^{11}C]DPA713 BP_{ND} in the AD group were significantly higher than those in both the young and elderly subjects in all ROIs. Despite the higher level of [^{11}C]DPA713 BP_{ND} in the elderly group, a significant difference was not observed between the young and elderly subjects in any ROIs (Figure 1(a) and supplementary figure 5). As reported previously,[12] the precuneus showed significantly higher [^{11}C](*R*)PK11195 BP_{ND} in AD patients than in elderly subjects. There was no significant difference in the levels of [^{11}C](*R*)PK11195 BP_{ND} between young and elderly subjects in all ROIs (Figure 1(b) and supplementary figure 6). [^{11}C]DPA713 and [^{11}C](*R*)PK11195 time-activity curves (TACs) for all three groups in the precuneus were shown in Figure 2. The horizontal axis in Figure 2 indicates the time. The vertical axes indicate %dose/L in Figure 2(a), and in Figure 2(b), they indicate a unitless ratio that was calculated by dividing the value of each TAC by the peak value of the same TAC. [^{11}C]DPA713 uptake reached a peak at 450 s, and [^{11}C](*R*)PK11195 uptake reached a peak at 75 s after tracer injection. Normalized input curves derived from young subjects for [^{11}C]DPA713 and [^{11}C](*R*)PK11195 are also shown in supplementary figure 7. BP_{ND} ratios of [^{11}C]DPA713 (AD BP_{ND}/elderly BP_{ND}) tended to be higher, especially in the brain regions outside the precuneus, compared with those of [^{11}C](*R*)PK11195 in AD patients (Figure 3 and supplementary figure 8), indicating that [^{11}C]DPA713 might be better for the delineation of microglial activation in the cerebral cortex than [^{11}C](*R*)PK11195. By contrast, a small difference in the ratios in the precuneus confirms that microglial activation is easily detected in this region in AD patients.

Correlation analysis

Pearson's correlation analysis showed significant negative correlations between [^{11}C]DPA713 BP_{ND} levels and MMSE scores among elderly subjects and AD patients in the caudate nucleus ($r = -0.64$, $p < 0.05$ corrected), pcc ($r = -0.68$, $p < 0.05$ corrected), precuneus ($r = -0.66$, $p < 0.05$ corrected), sfc ($r = -0.65$, $p < 0.05$ corrected), mfc ($r = -0.67$, $p < 0.05$ corrected), lateral temporal cortex ($r = -0.74$, $p < 0.05$ corrected), and occipital cortex ($r = -0.67$, $p < 0.05$ corrected) (Figure 4

and supplementary figure 9). In the rest of the ROIs, there were tendencies toward a negative correlation between [^{11}C]DPA713 BP levels and MMSE scores among elderly subjects and AD patients (supplementary figure 9). However, no significant correlations were found within each group consisting of either elderly subjects or AD patients, possibly because the cognitive levels within each group might not have been diversified enough to reach significance (supplementary figures 10 and 11). By contrast, no significant correlations between [^{11}C](*R*)PK11195 BP_{ND} levels and MMSE scores were found, with a tendency toward a negative correlation in the precuneus (data not shown).

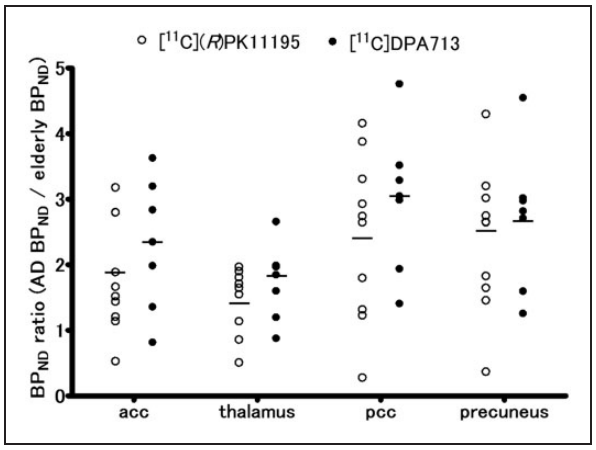

Figure 3. Representative scatter plots of regional BP_{ND} ratios of [^{11}C]DPA713 and [^{11}C](*R*)PK11195 (AD BP_{ND}/elderly BP_{ND}). [^{11}C]DPA713 BP_{ND} ratios tend to be higher than the [^{11}C](*R*)PK11195 BP_{ND} ratios in extensive brain regions.

SPM analysis

Figure 5(a) shows individual parametric PET images of [^{11}C]DPA713 BP_{ND} and [^{11}C](*R*)PK11195 BP_{ND} obtained from a young and an elderly subject as well as an AD patient. As observed in the [^{11}C]DPA713 PET images, an AD patient has a higher level of BP_{ND} than a young or an elderly subject. Regarding the [^{11}C](*R*)PK11195 PET images, subtle changes in binding can be observed across the three groups. The results of the SPM analysis are shown in Figure 5(b) and Table 3. Significantly higher BP_{ND} values of [^{11}C]DPA713 in AD patients compared with elderly subjects were observed in almost all brain regions as supported by ROI analyses. In the medial parietal cortex, significantly higher BP_{ND} values of [^{11}C](*R*)PK11195 in AD patients than in elderly subjects were observed. Although the SPM analysis showed a significant aging effect on the binding of [^{11}C]DPA713 BP_{ND} in the frontal cortex, medial parietal cortex, and occipital cortex based on a comparison between two age-different groups, SPM regression analysis with age taken as a covariate failed to show a clear

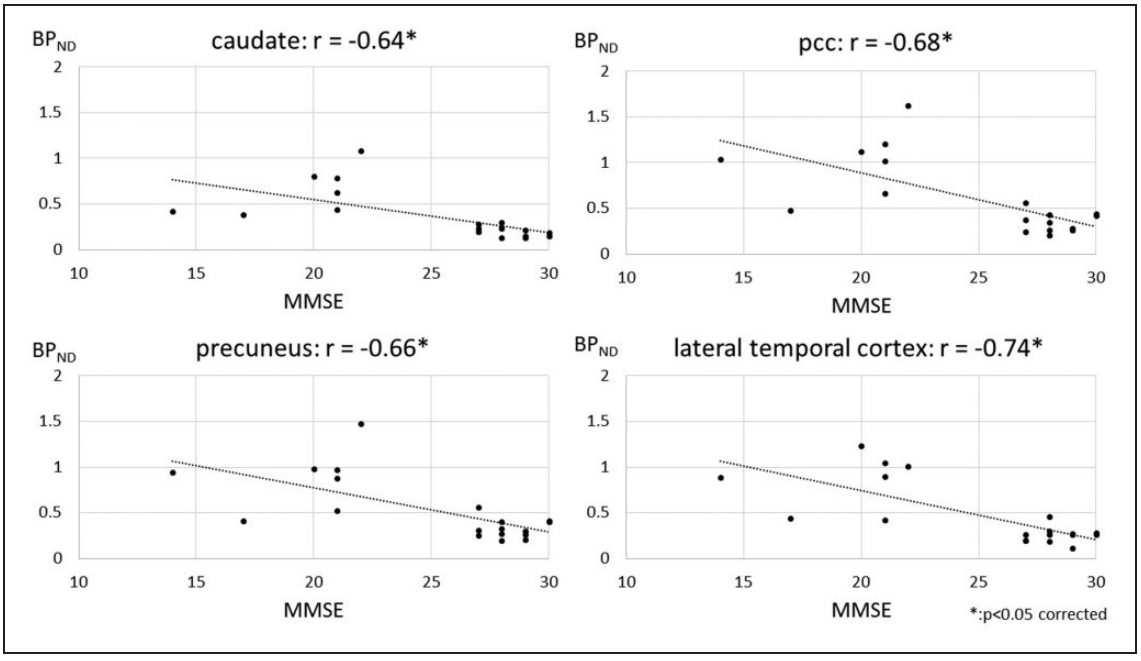

Figure 4. The relationship between [^{11}C]DPA713 binding with cognition. Statistically significant negative correlations between BP_{ND} values of [^{11}C]DPA713 and MMSE scores in extensive brain regions between elderly subjects and AD patients were observed. The asterisk (*) indicates $p < 0.05$, corrected for multiple comparisons.

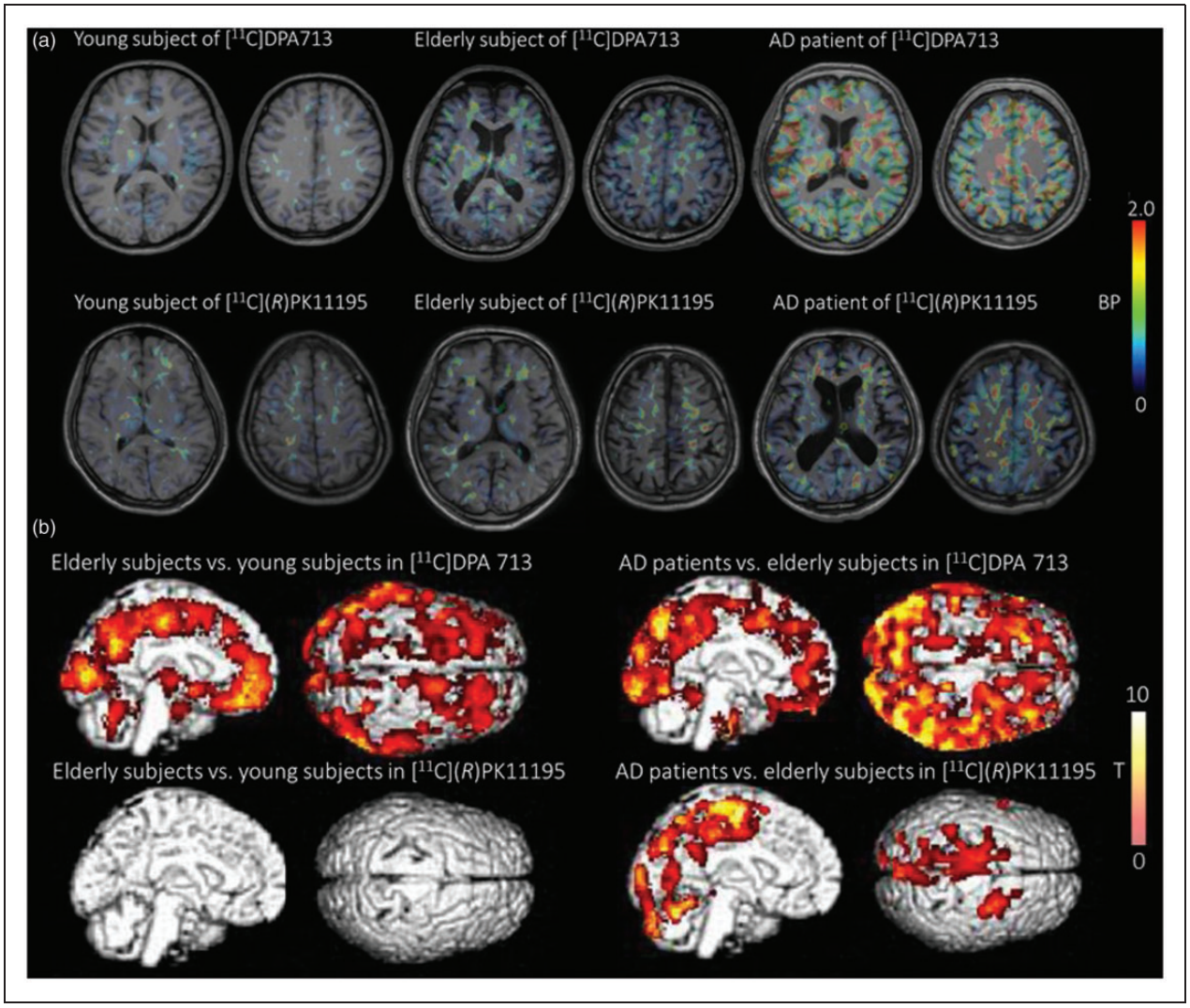

Figure 5. Illustration of BP_{ND} parametric images and results of a voxel wise analysis (SPM). A marked increase in the BP_{ND} level of [^{11}C]DPA713 (a, upper row) and a moderate elevation in [^{11}C](*R*)PK11195 BP_{ND} (a, lower row) are shown in AD patients compared with young and elderly subjects. SPM supported these findings (b).

association between age and TSPO binding at a significant level. There were no brain regions where [^{11}C](*R*)PK11195 BP_{ND} was significantly increased between young and elderly subjects.

Discussion

Microglial activation with normal aging by first- and second-generation TSPO tracers

The SPM analysis showed a significant increase in [^{11}C]DPA713 BP_{ND} over the greater number of brain regions in the elderly subjects compared with the young subjects (Figure 5(b) and Table 3). Our ROI analysis of [^{11}C]DPA713 showed a nonsignificant trend in BP_{ND} for all brain regions in elderly subjects when compared with young subjects, which was not observed for [^{11}C](*R*)PK11195 (Figure 1(a), Table 2, supplementary figure 5 and 6). By contrast, the ROI analysis of [^{11}C](*R*)PK11195 showed a negligible difference between young and elderly subjects in all ROIs (Figure 1(b), Table 2, and supplementary figure 6). Although the changes in [^{11}C]DPA713 binding failed to reach a significant level, possibly due to the small number of participants, the trend of higher [^{11}C]DPA713 BP_{ND} in elderly subjects might reflect age-related TSPO overexpression without regional preference in the healthy brain.

It has been reported that microglia in the rat brain were activated with age[4]; healthy older monkeys with cognitive impairments manifested highly activated microglia.[5] In vitro studies also reported increased activated microglia with normal aging.[2] It has been speculated that apoptosis and oxidative stress are responsible

for the activation of microglia during normal aging.[4,5] In previous PET studies, an increasing number of activated microglia measured by TSPO density have been described as a phenomenon accompanying normal aging of the brain.[14,20] Normal age-related cognitive decline in humans is associated with altered levels of proinflammatory cytokines, which might be mediated by activated microglia.[6] Various studies have normalized the activated microglia by pharmacological and dietary intervention and exercise, thus reducing neuroinflammatory responses.[31–33] Detecting the subtle increase in normal age-related microglial activation in younger subjects is beneficial to prevent the deleterious effects of cognitive impairment with normal aging.

Although [^{11}C](*R*)PK11195 has been shown to have a high affinity for TSPO from in vitro binding studies, in vivo imaging studies using [^{11}C](*R*)PK11195 to investigate neuroinflammatory processes showed poor signal-to-noise characteristics. Recently, TSPO PET studies have focused on identifying novel TSPO radioligands with high specific binding in vivo. Because our study showed that [^{11}C]DPA713 reveals a normal age-related increase in TSPO density in the greater number of brain regions compared with [^{11}C](*R*)PK11195, [^{11}C]DPA713 could be more suitable to detect the normal age-related changes in TSPO in healthy subjects.

Different bindings between [^{11}C]DPA713 and [^{11}C](R)PK11195

As shown in Figure 2(a) and supplementary figure 7A, peak values of TACs and normalized input curves were quite dispersed. The order of peak values in TACs from three groups was the same between [^{11}C]DPA713 and [^{11}C](*R*)PK11195 studies, i.e. the highest is the elderly TAC, followed by AD and young TACs in descending order. To facilitate visualization of the shape of TACs and normalized input curves, we compared the ratios of all curves as described in Figure 2(b) and supplementary figure 7B. [^{11}C]DPA713 uptake reached a peak later than [^{11}C](*R*)PK11195 uptake. The decline in [^{11}C]DPA713 uptake appears to be slower than that of [^{11}C](*R*)PK11195 uptake during the distribution phase. In the late phase, [^{11}C]DPA713 TACs were completely divided among the three groups (young, elderly, and AD subjects). By contrast, [^{11}C](*R*)PK11195 TACs seemed to be inseparable in the late phase. [^{11}C]DPA713 uptake did not reach a steady state compared with [^{11}C](*R*)PK11195 uptake. The longer scan time of [^{11}C]DPA713 would be appropriate for generation of BP_{ND} values under the steady state, our ROI and SPM analyses showed significant differences between the both tracers in the same scan protocol. Hence, the shorter scan time of [^{11}C]DPA713 in our study can be accepted as one benefit in reducing the burden of participants. Pharmacologically, the combination of a free receptor concentration (Bmax) and a ligand dissociation constant (Kd) or a ratio of Bmax/Kd is used as an index of binding potential for the ligand (tracer). Under the in vivo setting, however, nonspecific binding, radioligand metabolism, lipophilicity, and other factors affect this ratio, and each parameter cannot be separately determined. Taking into account, the results of our ROI and SPM analyses, a small slope in the distribution phase and a complete separation of the three groups in the late phase of [^{11}C]DPA713 TACs, rather than the difference of peak values in TACs, indicate that the specific binding of [^{11}C]DPA713 is greater than that of [^{11}C](*R*)PK11195.

This observation is supported by a previous animal study that showed a higher signal-to-noise ratio of [^{11}C]DPA713 than [^{11}C](*R*)PK11195 by direct comparison[23] as well as a human study with a small number of subjects that showed a trend toward better specific uptake of [^{11}C]DPA713 than [^{11}C](*R*)PK11195.[24] In our study, a larger but not statistically significant difference in the BP_{ND} ratio index (AD BP_{ND}/elderly BP_{ND}) was found in [^{11}C]DPA713 compared with [^{11}C](*R*)PK11195 (Figure 3 and supplementary figure 8). We conclude that [^{11}C]DPA713 can be more sensitive to TSPO than [^{11}C](*R*)PK11195.

Microglial activation in AD patients by first- and second-generation TSPO tracers

To our knowledge, this is the first [^{11}C]DPA713 PET study to evaluate the microglial activation measured by TSPO density in living AD brains. Our ROI analysis of [^{11}C]DPA713 showed that AD patients have significantly higher BP values in all ROIs than both young and elderly subjects (Figure 1(a), Table 2 and supplementary figure 5). Our ROI analysis of [^{11}C](*R*)PK11195 showed that AD patients have a significantly higher BP value than either young or elderly subjects only in the precuneus (Figure 1(b), Table 2 and supplementary figure 6). As shown in the Figure 1, supplementary figures 1, 3, and 5, our present method using the input curve from young subjects is adequate to compare the three groups (young subjects, elderly subjects, and AD patients) for [^{11}C]DPA713. By contrast, using the input curve from a clustered input curve could be more sensitive for [^{11}C](*R*)PK11195, because of the number of ROIs in which a significant difference between elderly subjects and AD patients (Figure 1, supplementary figure 2, 4 and 6). SPM analysis showed a significant increase of [^{11}C]DPA713 BP_{ND} in almost all brain regions and a significant increase of [^{11}C](*R*)PK11195 BP_{ND} in the medial parietal

Table 3. Results of SPM analysis.

	Cluster level ($p < 0.001$)		Peak level ($p < 0.001$)				
				Talairach coordinates			
	k_E	p value	Z value	x	y	z	Anatomical name
[^{11}C]DPA713							
AD patients vs. elderly subjects	84825	0.000	5.44	55	10	−18	Right superior temporal cortex, BA38
Elderly subjects vs. young subjects	60475	0.000	6.45	−22	−64	38	Left precuneus, BA7
			5.75	−54	−42	2	Left middle temporal gyrus, BA22
			5.57	−35	35	−2	Left inferior frontal gyrus, BA47
	386	0.001	4.79	14	−60	−44	Right cerebellum
[^{11}C](*R*)PK11195							
AD patients vs. elderly subjects	11169	0.000	4.77	28	4	54	Right superior frontal gyrus, BA6
			4.55	−2	−32	40	Left posterior cingulate gyrus, BA31
			4.29	−10	−8	58	Left superior frontal gyrus, BA6
	910	0.000	3.98	−54	12	32	Left inferior frontal gyrus, BA9
			3.93	−58	−10	52	Left postcentral gyrus, BA3
	627	0.000	4.09	−52	−56	−14	Left inferior temporal gyrus, BA20
			3.79	−54	−55	12	Left superior temporal gyrus, BA39
			3.55	−52	−62	5	Left middle temporal gyrus, BA37
Elderly subjects vs. young subjects	None		None				

cortex when comparing AD patients with elderly subjects (Figure 5(b) and Table 3). Although different AD groups were examined by different TSPO tracers, the same average MMSE scores between groups indicates that the current results of tracer binding can reflect the different specificities of the current tracers to the TSPO receptors in AD patients with similar pathologies. The medial parietal cortex is one of the pathophysiologically important regions in AD because glucose hypometabolism in this region is found at a very early stage of the disease.[34] Our previous study with [^{11}C](*R*)PK11195 PET was in line with this metabolic change, showing increased microglial activation measured by TSPO density in this region.[12] By contrast, [^{11}C]DPA713 binding appeared in larger brain regions, including the medial parietal region, suggesting that [^{11}C]DPA713 is a better tracer to detect the subtle changes in TSPO density at an early stage of AD.

Although TSPO is not only expressed in activated microglia but is also activated in astrocytes, an in vitro study suggested that TSPO is expressed largely in activated microglia.[35] In vivo detection of microglia using TSPO PET is indeed important in monitoring the presence of neuroinflammation in the brain. It is well known that activated microglia play both proinflammatory and anti-inflammatory roles in which M1 phenotype microglia are proinflammatory, leading to neuronal death,[7] and microglia with FCγ receptor II indicate an M2 phenotype[36] and play a role in neuroprotection by reducing β-amyloid in immunotherapies for AD.[37] The dichotomous distribution between M1- and M2-biased inflammatory profiles was observed in gene expression analysis (i.e. IL-1β, TNFα, etc.) in the postmortem brain of early AD patients (mean MMSE score 22.6).[36] Empirically, users of nonsteroidal anti-inflammatory drugs (NSAIDs) tend to have a lower risk of developing AD,[38] partly because NSAIDs decrease microglial activation, as shown in the AD mouse model.[39] A previous interventional study reported that NSAIDs are protective if initiated before the onset of AD symptoms but harmful after the development of cognitive impairment.[40] Latta et al. proposed that the differential effects of NSAIDs were caused by M1 or M2 inflammatory profiles.[9] Indeed, studies on agents acting on these phenotypes are currently being performed.[36] Thus, in vivo monitoring of microglial activation during the preclinical AD phase is

becoming increasingly significant with the uses of a high-sensitivity tracer such as [^{11}C]DPA713, whereas [^{11}C]DPA713 would not be expected to differentiate between these M1 from M2 microglia.

Clinical significance of [^{11}C]DPA713 and [^{11}C](R)PK11195 binding in AD

There were significant negative correlations between [^{11}C]DPA713 BP_{ND} values and MMSE scores among elderly subjects and AD patients in the caudate nucleus, pcc, precuneus, sfc, mfc, lateral temporal cortex and occipital cortex, and the rest of the ROIs showed a tendency toward a negative correlation (Figure 4, and supplementary figure 9). By contrast, [^{11}C](*R*)PK11195 BP_{ND} values did not correlate significantly with MMSE scores among elderly subjects and AD patients (data not shown).

In the present study, because of a small variation in MMSE scores within the small AD group, the clinical–molecular binding relationship was examined by grouping the data from elderly subjects and AD patients. This resulted in a stronger correlation ($r = -0.56$ to -0.74) between TSPO overexpression and cognitive decline than in previous [^{11}C]PBR28 PET studies among AD patients ($r = -0.35$ to -0.50). Because TSPO overexpression occurs during the mild cognitive impairment (MCI) phase,[41] a mixture of MCI data may further improve the correlation coefficient. Specifically considering AD pathology, any information on β-amyloid deposition among healthy and MCI subjects can add pathophysiological relevance to the changes in microglial activation measured by the TSPO PET study through normal aging or early AD stages.

Other second-generation TSPO tracers in AD

Several second-generation TSPO tracers have been used in studies with [^{11}C]DAA1106, [^{11}C]vinpocetine, [^{11}C]PBR28, [^{18}F]FEDDA, and [^{18}F]DPA714 in AD patients, showing mixed results.[18–22] Among them, the [^{11}C]DAA1106 and [^{11}C]PBR28 studies reported that TSPO density significantly increased in AD patients, and the [^{11}C]PBR28 study only showed a significant correlation with cognitive severity in AD patients.[18,19] [^{11}C]DAA1106 and [^{11}C]PBR28 had a ~10-fold higher affinity ($Ki = 2.8 \pm 0.3$ nM, and 3.4 ± 0.2 nM, respectively) compared with [^{11}C]DPA713 and [^{11}C](*R*)PK11195 ($Ki = 15.0 \pm 2.2$ nM and 28.3 ± 4.0 nM, respectively) in an in vitro examination.[42] Although the sample size of our study ($n = 7$) is smaller than in previous [^{11}C]DAA1106 and [^{11}C]PBR28 studies ($n = 10$ and 19, respectively), and the analytic approach of our study (TSPO density estimated by SRTM using the input curve from young subjects without arterial blood sampling) is methodologically different from both the [^{11}C]DAA1106 and [^{11}C]PBR28 studies (TSPO density estimated by two tissue compartment model using input curve from elderly subjects with arterial blood sampling), our [^{11}C]DPA713 study showed the increased TSPO density in AD patients in a greater number of regions than the previous [^{11}C]DAA1106 and [^{11}C]PBR28 studies. Thus, it can currently be stated that [^{11}C]DPA713 might be more suitable for in vivo delineation of TSPO density among second-generation TSPO tracers in neurological disorders.

Gene issue on TSPO tracers

Recent in vitro studies reported substantial heterogeneity in the affinity of the second-generation TSPO candidate tracers.[42] Based on the genotypes of the tracers for their affinity, people can reportedly be categorized into three subgroups: high-affinity binders (HABs) and low-affinity binders (LABs) who express a single binding site for TSPO with either high or low affinity, respectively, and mixed-affinity binders (MABs) who express approximately equal numbers of the HAB and LAB binding sites.[42] This differential affinity is caused by the rs6971 polymorphism on the TSPO gene.[25] [^{11}C](*R*)PK11195 binding in the brain does not exhibit sensitivity to the rs6971 polymorphism. We did not obtain genomic DNA from all subjects, because it has been reported that the rs6971 polymorphism is rare in Asian populations, including among Japanese (~4% allelic frequency) (http://hapmap.ncbi.nlm.nih.gov/cgi-perl/snp_details_phase3?name=rs6971&source=hapmap28_B36&tmpl=snp_details_phase3).[25] Because all subjects in our study were Japanese, it is unlikely that the gene polymorphism issue affects the present interpretation of the tracer sensitivity of [^{11}C](*R*)PK11195 and [^{11}C]DPA713.

Conclusion

The results from this study show that [^{11}C]DPA713 detects increased TSPO density related to the normal aging and AD stages in more extensive regions of the brain than [^{11}C](*R*)PK11195 or other second-generation TSPO tracers. A major limitation in our study is that we did not directly compare the binding capacity of [^{11}C]DPA713 with that of [^{11}C](*R*)PK11195 in the same subjects. However, the accumulated evidence and the robust statistical evaluations in our study allow us to confirm the advantage of using [^{11}C]DPA713 for detecting microgliosis in the living brain. The use of this tracer would also help to monitor changes in microglial activation measured by TSPO overexpression during any preclinical states of neurological and psychiatric disorders.

Funding

The author(s) disclosed receipt of the following financial support for the research, authorship, and/or publication of this article: This work was supported by a Research Grant for Longevity Science from the Ministry of Health, Labor and Welfare of Japan, and Scientific Research from the Ministry of Education, Culture, Sports, Science, and Technology of Japan.

Acknowledgments

The authors thank Mr. Toshihiko Kanno (Hamamatsu Photonics Medical Foundation) for his support.

Declaration of conflicting interests

The author(s) declared no potential conflicts of interest with respect to the research, authorship, and/or publication of this article.

Authors' contributions

MY, NM, and YO designed the study. MY and YO wrote the paper. MY, TT, TB, KN, KT, YI, EY, KS, and YO analyzed the data. MF synthesized the tracers.

Supplementary material

Supplementary material for this paper can be found at http://jcbfm.sagepub.com/content/by/supplemental-data

References

1. Gulyas B, Makkai B, Kasa P, et al. A comparative autoradiography study in post mortem whole hemisphere human brain slices taken from Alzheimer patients and age-matched controls using two radiolabelled DAA1106 analogues with high affinity to the peripheral benzodiazepine receptor (PBR) system. *Neurochem Int* 2009; 54: 28–36.
2. Sheng JG, Mrak RE and Griffin WS. Enlarged and phagocytic, but not primed, interleukin-1 alpha-immunoreactive microglia increase with age in normal human brain. *Acta Neuropathol* 1998; 95: 229–234.
3. Venneti S, Wiley CA and Kofler J. Imaging microglial activation during neuroinflammation and Alzheimer's disease. *J Neuroimmune Pharmacol: Off J Soc NeuroImmune Pharmacol* 2009; 4: 227–243.
4. Frank MG, Barrientos RM, Watkins LR, et al. Aging sensitizes rapidly isolated hippocampal microglia to LPS ex vivo. *J Neuroimmunol* 2010; 226: 181–184.
5. Sloane JA, Hollander W, Moss MB, et al. Increased microglial activation and protein nitration in white matter of the aging monkey. *Neurobiol Aging* 1999; 20: 395–405.
6. Lekander M, von Essen J, Schultzberg M, et al. Cytokines and memory across the mature life span of women. *Scand J Psychol* 2011; 52: 229–235.
7. McGeer EG and McGeer PL. The importance of inflammatory mechanisms in Alzheimer disease. *Exp Gerontol* 1998; 33: 371–378.
8. Barrientos RM, Kitt MM, Watkins LR, et al. Neuroinflammation in the normal aging hippocampus. *Neuroscience* 2015; 309: 84–99.
9. Latta CH, Brothers HM and Wilcock DM. Neuroinflammation in Alzheimer's disease: A source of heterogeneity and target for personalized therapy. *Neuroscience* 2015; 302: 103–111.
10. Suzuki K, Sugihara G, Ouchi Y, et al. Microglial activation in young adults with autism spectrum disorder. *JAMA Psychiatr* 2013; 70: 49–58.
11. Venneti S, Wang G, Nguyen J, et al. The positron emission tomography ligand DAA1106 binds with high affinity to activated microglia in human neurological disorders. *J Neuropathol Exp Neurol* 2008; 67: 1001–1010.
12. Yokokura M, Mori N, Yagi S, et al. In vivo changes in microglial activation and amyloid deposits in brain regions with hypometabolism in Alzheimer's disease. *Eur J Nucl Med Mol Imaging* 2011; 38: 343–351.
13. Ouchi Y, Yoshikawa E, Sekine Y, et al. Microglial activation and dopamine terminal loss in early Parkinson's disease. *Ann Neurol* 2005; 57: 168–175.
14. Kumar A, Muzik O, Shandal V, et al. Evaluation of age-related changes in translocator protein (TSPO) in human brain using (11)C-[R]-PK11195 PET. *J Neuroinflam* 2012; 9: 232–241.
15. Cagnin A, Brooks DJ, Kennedy AM, et al. In-vivo measurement of activated microglia in dementia. *Lancet* 2001; 358: 461–467.
16. Wiley CA, Lopresti BJ, Venneti S, et al. Carbon 11-labeled Pittsburgh Compound B and carbon 11-labeled (R)-PK11195 positron emission tomographic imaging in Alzheimer disease. *Arch Neurol* 2009; 66: 60–67.
17. Schuitemaker A, Kropholler MA, Boellaard R, et al. Microglial activation in Alzheimer's disease: an (R)-[(1)(1)C]PK11195 positron emission tomography study. *Neurobiol Aging* 2013; 34: 128–136.
18. Yasuno F, Ota M, Kosaka J, et al. Increased binding of peripheral benzodiazepine receptor in Alzheimer's disease measured by positron emission tomography with [11C]DAA1106. *Biol Psychiatry* 2008; 64: 835–841.
19. Kreisl WC, Lyoo CH, McGwier M, et al. In vivo radioligand binding to translocator protein correlates with severity of Alzheimer's disease. *Brain* 2013; 136: 2228–2238.
20. Gulyas B, Vas A, Toth M, et al. Age and disease related changes in the translocator protein (TSPO) system in the human brain: positron emission tomography measurements with [11C]vinpocetine. *Neuroimage* 2011; 56: 1111–1121.
21. Varrone A, Mattsson P, Forsberg A, et al. In vivo imaging of the 18-kDa translocator protein (TSPO) with [18F]FEDAA1106 and PET does not show increased binding in Alzheimer's disease patients. *Eur J Nucl Med Mol Imaging* 2013; 40: 921–931.
22. Golla SS, Boellaard R, Oikonen V, et al. Quantification of [18F]DPA-714 binding in the human brain: initial studies in healthy controls and Alzheimer's disease patients. *J Cereb Blood Flow Metab* 2015; 35: 766–772.

23. Boutin H, Chauveau F, Thominiaux C, et al. 11C-DPA-713: a novel peripheral benzodiazepine receptor PET ligand for in vivo imaging of neuroinflammation. *J Nucl Med* 2007; 48: 573–581.
24. Endres CJ, Pomper MG, James M, et al. Initial evaluation of 11C-DPA-713, a novel TSPO PET ligand, in humans. *J Nucl Med* 2009; 50: 1276–1282.
25. Owen DR, Yeo AJ, Gunn RN, et al. An 18-kDa translocator protein (TSPO) polymorphism explains differences in binding affinity of the PET radioligand PBR28. *J Cereb Blood Flow Metab* 2012; 32: 1–5.
26. McKhann G, Drachman D, Folstein M, et al. Clinical diagnosis of Alzheimer's disease: report of the NINCDS-ADRDA Work Group under the auspices of Department of Health and Human Services Task Force on Alzheimer's Disease. *Neurology* 1984; 34: 939–944.
27. Ouchi Y, Nobezawa S, Okada H, et al. Altered glucose metabolism in the hippocampal head in memory impairment. *Neurology* 1998; 51: 136–142.
28. Watanabe M, Shimizu K, Omura T, et al. A new high-resolution PET scanner dedicated to brain research. *IEEE Trans Nucl Sci* 2002; 49: 634–639.
29. Lammertsma AA and Hume SP. Simplified reference tissue model for PET receptor studies. *Neuroimage* 1996; 4: 153–158.
30. Ashburner J, Haslam J, Taylor C, et al. *A cluster analysis approach for the characterization of dynamic PET data. Quantification of brain function using PET*. San Diego: Academic Press, 1996, pp.301–306.
31. Barrientos RM, Hein AM, Frank MG, et al. Intracisternal interleukin-1 receptor antagonist prevents postoperative cognitive decline and neuroinflammatory response in aged rats. *J Neurosci* 2012; 32: 14641–14648.
32. Abraham J and Johnson RW. Consuming a diet supplemented with resveratrol reduced infection-related neuroinflammation and deficits in working memory in aged mice. *Rejuvenation Res* 2009; 12: 445–453.
33. Barrientos RM, Frank MG, Crysdale NY, et al. Little exercise, big effects: reversing aging and infection-induced memory deficits, and underlying processes. *J Neurosci* 2011; 31: 11578–11586.
34. Minoshima S, Giordani B, Berent S, et al. Metabolic reduction in the posterior cingulate cortex in very early Alzheimer's disease. *Ann Neurol* 1997; 42: 85–94.
35. Dickens AM, Vainio S, Marjamaki P, et al. Detection of microglial activation in an acute model of neuroinflammation using PET and radiotracers 11C-(R)-PK11195 and 18F-GE-180. *J Nucl Med* 2014; 55: 466–472.
36. Sudduth TL, Schmitt FA, Nelson PT, et al. Neuroinflammatory phenotype in early Alzheimer's disease. *Neurobiol Aging* 2013; 34: 1051–1059.
37. Wilcock DM, Rojiani A, Rosenthal A, et al. Passive amyloid immunotherapy clears amyloid and transiently activates microglia in a transgenic mouse model of amyloid deposition. *J Neurosci* 2004; 24: 6144–6151.
38. McGeer PL and McGeer EG. NSAIDs and Alzheimer disease: epidemiological, animal model and clinical studies. *Neurobiol Aging* 2007; 28: 639–647.
39. Lim GP, Yang F, Chu T, et al. Ibuprofen suppresses plaque pathology and inflammation in a mouse model for Alzheimer's disease. *J Neurosci* 2000; 20: 5709–5714.
40. Breitner JC, Baker LD, Montine TJ, et al. Extended results of the Alzheimer's disease anti-inflammatory prevention trial. *Alzheimers Dement* 2011; 7: 402–411.
41. Yasuno F, Kosaka J, Ota M, et al. Increased binding of peripheral benzodiazepine receptor in mild cognitive impairment-dementia converters measured by positron emission tomography with [(1)(1)C]DAA1106. *Psychiatr Res* 2012; 203: 67–74.
42. Owen DR, Gunn RN, Rabiner EA, et al. Mixed-affinity binding in humans with 18-kDa translocator protein ligands. *J Nucl Med* 2011; 52: 24–32.